

## Deoxygenation Performance of Polydimethylsiloxane Mixed-Matrix Membranes for Dissolved Oxygen Removal from Water

Ting Li,<sup>1,2</sup> Ping Yu,<sup>1</sup> Yunbai Luo<sup>1</sup>

<sup>1</sup>College of Chemistry and Molecular Sciences, Wuhan University, Wuhan 430072, Hubei, People's Republic of China

<sup>2</sup>Suzhou Nuclear Power Research Institute Company, Limited, Shenzhen 518000, Guangdong, People's Republic of China

Correspondence to: P. Yu (E-mail: yuping@whu.edu.cn)

**ABSTRACT:** The removal of dissolved oxygen (DO) from water is an essential and important step in many industrial applications. The membrane technique offers much potential superiority over conventional physical and chemical processes. The development of a high-performance membrane is the core of the membrane separation technique. In this study, a crosslinked matrix composed of a polydimethylsiloxane (PDMS) membrane with incorporated silica networks by the sol-gel method was manufactured. The application of the membrane method for the removal of DO from water on the laboratory scale was studied. The membrane properties and morphological structure were characterized by Fourier transform infrared spectroscopy, scanning electron microscopy, crosslinking density, and mechanical measurements. The PDMS hybrid membranes on the deoxygenation experiment by a vacuum degassing process were investigated. The results show that the crosslinked PDMS hybrid membranes effectively improved the oxygen-removal efficiency with increasing tetraethoxysilane (TEOS) content, and the best performance was obtained when the weight ratio of PDMS-TEOS concentrations was 10:5. The optimal conditions for the deoxygenation performance were also investigated, and the results indicate that the degassing performances were related to the operating temperature, vacuum level, and feed flow rate. The PDMS nonporous composite membranes showed superior performances and have good potential for applications in industry for the removal of DO from water. © 2014 Wiley Periodicals, Inc. *J. Appl. Polym. Sci.* **2015**, *132*, 41350.

**KEYWORDS:** crosslinking; membranes; nanoparticles; nanowires and nanocrystals; properties and characterization; rubber

Received 2 March 2014; accepted 28 July 2014

DOI: 10.1002/app.41350

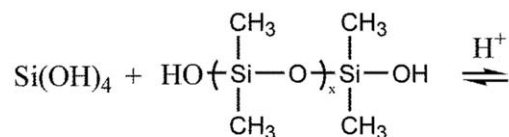
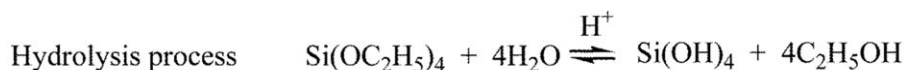
### INTRODUCTION

Dissolved oxygen (DO) is oxygen molecules from ambient air dissolved in water. The DO has strong oxidative properties under high temperature and high pressure; this readily accelerates metal oxidation and corrosion and has adverse effects in industrial applications. The removal of DO from water is a necessary processes that is applied in various industries; this includes semiconductor manufacturing, power plants, food, and pharmaceutical productions.<sup>1–3</sup> For instance, a desired DO concentration in water on the parts per billion level has been stipulated for boiler feed water in power plants.<sup>4,5</sup> In the semiconductor process, the concentration of DO in ultrapure rinse water is also controlled strictly as it can result in the growth of undesirable native silica oxide.<sup>6,7</sup> All of these reasons establish industrial importance for the removal of DO from water.

There are several traditional methods used for DO removal; these include thermal degassing, vacuum degassing, purging with nitrogen, and oxidation-reduction reaction by the addition of sodium sulfite or hydrazine.<sup>5</sup> The conventional physical methods often have bulky

constructions and high operating costs, and the chemical methods are not very desirable because of problems in changing the water quality affected by the reducing agents (e.g., toxicity or the ionic content of water). Nowadays, the membrane process has attracted more and more attention because of its great advantages over conventional deoxygenation processes;<sup>8–11</sup> these advantages include a faster mass-transfer efficiency, larger surface area per unit volume, tighter modular construction, environmental protection, higher efficiency, and lower energy costs.<sup>12–15</sup> These unique properties make the membrane method a competitive new technology compared to traditional technologies in achieving mass transfer between two phases. Gradually, the membrane method has become an attractive and competitive choice for the removal of dissolved components from water.<sup>16,17</sup> Membrane contactors have been applied to different processes in liquid-gas membrane separation technology.<sup>18–20</sup>

In membrane degassing, the membrane provides the liquid-gas mass-transfer interface. Water is fed on one side of the membrane module and a vacuum is applied on the other side. With the vacuum, the partial pressure difference of oxygen drives the



Condensation process

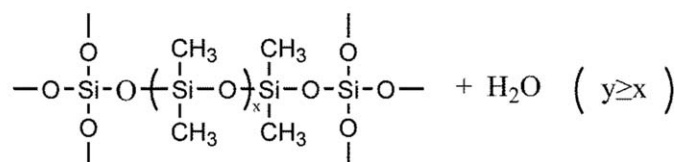


Figure 1. Interaction between TEOS and PDMS.

oxygen permeation rate through the membrane, and the difference in the partial pressure of vapor drives vapor permeation.<sup>21</sup> When the deoxygenation membrane has a dense layer and a nonporous structure, the process is described by the solution–diffusion model. It is held that the mass-transport process consists of three fundamental processes: (1) selective sorption into the membrane top layer, (2) diffusion of the dissolved species across the membrane matrix, and (3) desorption and diffusion to the permeate side of the membrane with a vacuum. The core of the membrane separation technique is the fabrication of a high-performance membrane and the choice of the correct membrane material. For many years, a lot of attention has been paid to polydimethylsiloxane (PDMS) as one of the most widely used membrane materials for gas separation.<sup>22,23</sup> PDMS can be crosslinked into networks, and the elastomer has excellent permeability to small molecules;<sup>24,25</sup> this is attributed to its large free volume from the high flexibility of the siloxane (—Si—O—) chains. Therefore, PDMS could be a suitable membrane material for oxygen permeation.

However, the pure PDMS membrane often has a relatively low permselectivity and poor mechanical strength. Various modifications have been attempted to enhance the selectivity and membrane-forming ability of elastomeric PDMS to acquire better and wider applications; these include filling, grafting, crosslinking, blending, and copolymerization. In recent years, PDMS has been used widely to manufacture polymer–inorganic hybrid membranes.<sup>26–29</sup> The introduction of inorganic fillers into elastomers in many cases could significantly improve the properties of the membranes because of the intermolecular interactions between inorganic and organic materials.<sup>30–33</sup> For this purpose, inorganic fillers have been introduced into the backbone of PDMS. The common methods for fabricating PDMS hybrid membranes include physical blending and the sol–gel method.<sup>34–37</sup>

Over the past several years, research in membrane technology for the deoxygenation process has focused mainly on the improvement of design membrane modules and devices; research on the fabrication of high-performance membranes for DO removal from water has been less studied.<sup>38–40</sup> The main objective of this

study was to develop high-performance membranes for the deoxygenation process and to improve the DO-removal efficiency. The PDMS matrix membranes in this study were prepared by the incorporation of organic polymers with alkoxy silanes. In this study, tetraethoxysilane (TEOS) was used as a silica precursor to prepare PDMS–silica mixed-matrix membranes. The idea of the incorporation of TEOS was based on the similar structure of PDMS, which consists of Si—O—Si bonds, to that of silica gel. The sol–gel method started from a homogeneous solution, gave better control of the mixed-matrix membrane, and prevented the problems of mechanical blending. By properly controlling the hydrolysis and condensation reactions of TEOS in the presence of a preformed organic polymer, we found it to be possible to obtain highly permeable and permselective PDMS matrix membranes. The membranes were characterized by Fourier transform infrared (FTIR) spectroscopy, scanning electron microscopy (SEM), and thermal analysis. The membrane separation performance was evaluated by the deoxygenation process on a laboratory scale. The effects of the feed temperature, feed flow rate, and operating vacuum level on the membrane performance were examined.

## EXPERIMENTAL

### Materials

TEOS, ethanol, hydrochloric acid, *n*-heptane, and dibutyltin dilaurate were obtained from Sinopharm Chemical Reagent Co., Ltd. (China). The hydroxyl-terminated PDMS {HO—[Si(CH<sub>3</sub>)<sub>2</sub>O]<sub>n</sub>—H; the corresponding average molecular weight was 3.6 × 10<sup>5</sup> g/mol} was purchased from Beijing Chemical Co. (China). The poly(vinylidene fluoride) ultrafiltration membranes were from China Development Center of Water Treatment Technology and were used as the supporting layer. All of the other reagents were analytical grade and were used without further purification. Deionized water from a Millipore ultrapure water system was used in all of the experiments.

### Preparation of the PDMS Mixed-Matrix Membranes

For the sol–gel chemistry, TEOS was used as a precursor. TEOS was previously diluted in ethanol and then added to PDMS under magnetic stirring at room temperature. An HCl solution was dropped into the PDMS–TEOS mixed solution to adjust

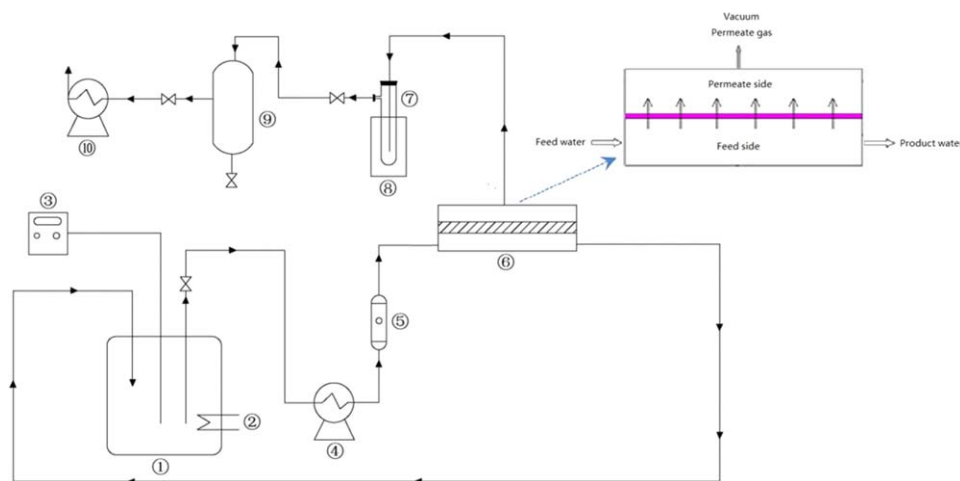


**Figure 2.** Schematic diagram of the experimental apparatus for DO removal: (1) feed tank, (2) heating unit, (3) DO meter, (4) flow control pump, (5) rotameter, (6) membrane cell, (7) collecting bottle, (8) liquid nitrogen cold trap, (9) buffer vessel, and (10) vacuum pump. [Color figure can be viewed in the online issue, which is available at [wileyonlinelibrary.com](http://wileyonlinelibrary.com).]

the pH at 4.5 and maintain the hydrolysis reaction for 30 min. Then, a small amount of dibutyltin dilaurate was added to the solutions; this served as a catalyst for the crosslinking reaction of PDMS and TEOS. After undergoing 24 h of the crosslinking reaction, the solutions were kept in a vacuum oven to remove air bubbles. Then, they were cast onto a poly(vinylidene fluoride) porous support membrane at room temperature. The membranes were kept *in vacuo* at 80°C for 24 h to accomplish a deep crosslinking process and evaporate the solvent. All of the samples were stored in a dust-free and dry environment before the deoxygenation measurements. The interaction between TEOS and PDMS mainly included hydrolysis and condensation reactions. As shown in Figure 1, an approach that combined the polymerization of PDMS with silica precipitation was developed to prepare the PDMS mixed-matrix membranes. TEOS served not only as the silicon precursor but also as the crosslinking agent for PDMS. To obtain various hybrid membranes with different SiO<sub>2</sub> contents, the weight ratio between PDMS and TEOS was changed to 10:1, 10:2, 10:3, 10:4, 10:5, and 10:6. Those samples were designated as PDMS-1, PDMS-2, PDMS-3, PDMS-4, PDMS-5, and PDMS-6, respectively.

#### Characterization of the PDMS Mixed-Matrix Membranes

**FTIR Analysis.** The attenuated total reflectance (ATR)-FTIR spectrum was measured with a Nicolet Avatar 360 FTIR spectrophotometer in the scanning range 4000–500 cm<sup>-1</sup>.

**Morphological Analysis.** The surface morphology of the PDMS hybrid membranes was observed with SEM (FEI Quanta 200, Holland). The membranes were sputter-coated with a thin film of gold.

**Crosslinking Density and Swelling Degree (SD) Measurements.** The crosslinking density and SD values of the membrane were determined by the equilibrium swelling method. The crosslinking density was based on the swelling of rubber in a solvent at equilibrium; the diffusion rate of the solvent molecules into the crosslinking network was equal to the effusion rate. The dry PDMS hybrid membranes were immersed in

heptane at 25°C until equilibrium swelling was reached. The membranes samples were weighed carefully before and after they were swollen. All of the obtained values were the average of five different measurements.

The crosslinking density was calculated according to the Flory–Rehner equation:<sup>41</sup>

$$v_e = - \frac{\ln(1-v_2) + v_2 + \chi v_2^2}{v(v_2^{1/3} - v_2/2)} \quad (1)$$

where  $v_e$  is the crosslinking density of the membrane (mol/cm<sup>3</sup>),  $v$  is the molar volume of heptane (cm<sup>3</sup> mol),  $\chi$  is the interaction parameter between PDMS and heptane (0.49 in this study), and  $v_2$  is the volume fraction of the PDMS membrane.

$v_2$  was calculated by eq. (2):

$$v_2 = \frac{w_1/\rho_1}{\frac{(w_1-w_2)}{\rho_1} + w_1/\rho_1} \times 100\% \quad (2)$$

where  $\rho_1$  and  $\rho_2$  are the densities of the PDMS and heptane (g/m<sup>3</sup>), respectively, and  $W_1$  and  $W_2$  are the weights of the dried and swollen membranes (g), respectively.

The SD of the dense membrane was calculated by eq. (3):

$$SD = \frac{w_2 - w_1}{w_1} \times 100\% \quad (3)$$

**Mechanical Properties.** The mechanical properties of the PDMS mixed-matrix membranes in the dry state were measured on a universal testing machine (CMT6350, Shenzhen SANS Test Machine Co., Ltd., China). The samples were tested at least three times, and the average value was recorded. The measurements were carried out at room temperature with a rate of pull of 2 mm/min.

#### Performance of the Membranes in DO Removal

The DO-removal experiments were conducted on a laboratory-scale circulating unit, as shown in Figure 2. The membrane was installed in a stainless membrane cell with an effective surface

area of 51.35 cm<sup>2</sup> in contact with the feed water. The feed water saturated with DO was continuously circulated through a micropump. The vacuum was exerted on the membrane unit by a vacuum pump. The water was pumped instantly through the downstream side of the membrane cell while the vacuum was applied at the upstream side to pull oxygen out of the water. The performances of membranes were determined by the continuous observation and analysis of the DO concentrations in the feed water with a DO meter (HQ30d, HACH Co.). During the deoxygenation experimental runs, the DO concentrations were measured over a predetermined time after the system temperatures reached steady state. The volume of the feed tank was 5.2 L, and the weight of oxygen removal from water could be calculated by the differences in the DO concentrations in the feed tank because it was a sealed system.

The permeation flux of oxygen ( $J_o$ ; g m<sup>-2</sup> h<sup>-1</sup>) and the permeation flux of water ( $J_w$ ; g m<sup>-2</sup> h<sup>-1</sup>) were calculated by eqs. (4) and (5), respectively:

$$J_o (\text{g/m}^2 \text{h}) = \frac{Q}{A \Delta T} \quad (4)$$

$$J_w (\text{g/m}^2 \text{h}) = \frac{Q_w}{A \Delta T} \quad (5)$$

where  $Q$  is the weight of oxygen removed (g) over a predetermined time,  $\Delta T$  is the run time of the DO-removal process (h), and  $A$  is the effective membrane area (m<sup>2</sup>).

The separation factor ( $\alpha$ ) was calculated by eq. (6):

$$\alpha = \frac{y_{\text{oxygen}}/y_{\text{water}}}{x_{\text{oxygen}}/w_{\text{water}}} \quad (6)$$

where  $x_{\text{oxygen}}$ ,  $x_{\text{water}}$ ,  $y_{\text{oxygen}}$ , and  $y_{\text{water}}$  are the molar fractions of oxygen and water in the feed and permeate, respectively.

To investigate the effect of the PDMS hybrid membranes and operating conditions on the DO-removal performance, the experimental variables in the study, including the TEOS content, feed water flow rate, operating temperature, and vacuum level, were included. All of the tests were repeated several times to ensure the repeatability of consequence, and a maximum fluctuation of 2% was obtained.

## RESULTS AND DISCUSSION

### Characterization of SiO<sub>2</sub> Particles and Hybrid Membranes

**FTIR Spectroscopy.** The structural characterization of the membranes was carried out by ATR-FTIR spectroscopy. The IR spectra of the PDMS mixed-matrix membranes with different TEOS contents are shown in Figure 3. As shown in Figure 3, the IR spectra was normalized corresponding to the vibration of the Si—O—Si bonds in the PDMS-silica networks. The absorption peak that was observed at 1010 cm<sup>-1</sup> in the spectrum was attributed to Si—O—Si symmetric stretching vibrations. The absorption peak at 787 cm<sup>-1</sup> was the symmetric stretching vibrations of the Si—O—Si groups. Furthermore, in a comparison of the different TEOS concentrations of the membranes, the spectra showed that the peak intensities of the Si—O—Si groups at 1010 and 787 cm<sup>-1</sup> were significantly enhanced when the silicon precursor content was increased; this indicated the formation of the hybrid network in the hybrid material and the

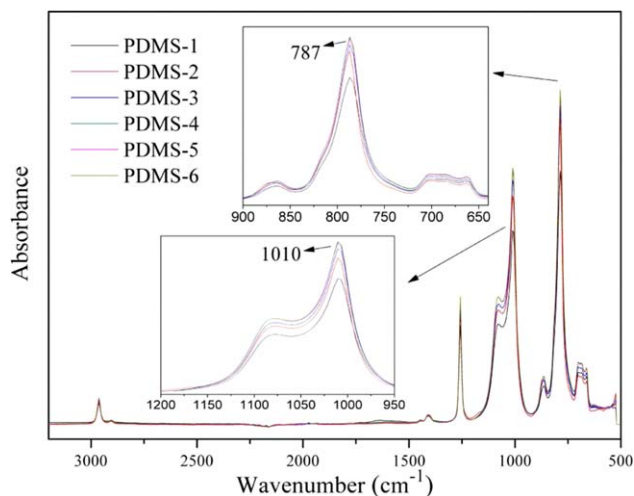


**Figure 3.** ATR-FTIR spectra of the PDMS hybrid membranes. [Color figure can be viewed in the online issue, which is available at [wileyonlinelibrary.com](http://wileyonlinelibrary.com).]

higher weight fraction of SiO<sub>2</sub> in the PDMS-silica mixed-matrix membranes. The characteristic absorption band of the Si—OH groups at 3300 and 950 cm<sup>-1</sup> did not appear in the spectrum, which indicated that most of the terminal hydroxyl groups of PDMS were removed during the crosslinking reaction. Therefore, the hydrolyzed TEOS already formed the three-dimensional Si—O—Si network.

**Morphological Analysis.** The characteristics of the surface morphologies of the PDMS mixed-matrix membranes with various TEOS contents are shown in Figure 4. As mentioned earlier, TEOS served as not only the silicon precursor but also the crosslinking agent for PDMS. When the TEOS concentration was lower, the TEOS mainly participated in the crosslinking process, reacted with PDMS, and formed the three-dimensional network. As shown in the SEM images in Figure 4(A–C), there was a general tendency for the membrane surface structures to become dense and smooth. When the TEOS concentration was higher, TEOS was involved in the sol-gel reaction and formed nanosilica particles within the PDMS matrix. The results show that the particles were homogeneously dispersed in the membrane matrix. Because of the flexible chains of the silicon rubber, the PDMS matrix network filled up the membrane defect immediately. The presence of TEOS promoted better mixing of the organic phase and inorganic phase, and the favorable compatibility between the PDMS matrix and the SiO<sub>2</sub> inorganic particles promoted the homogeneous dispersion.

**Crosslinking Density and SD Measurements.** The crosslinking density and SD were also important parameters for defining the properties of the membranes. Figure 5 displays the effect of the TEOS content on the crosslinking density and SD of the PDMS hybrid membranes. As shown in Figure 5, the crosslinking density in the PDMS-silica hybrid membranes increased remarkably with the addition of TEOS and then slightly increased with the increasing TEOS-PDMS ratio from 0.5 to 0.6. This means that TEOS contributed to the crosslinking process of the polymer networks; the silica particles provided a number of additional

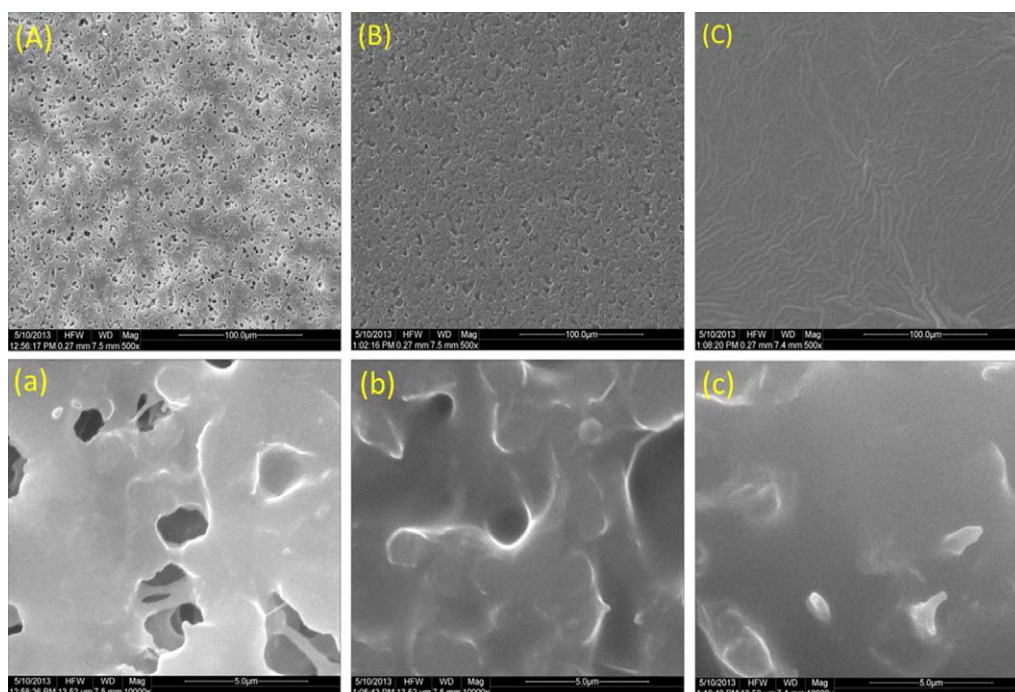


**Figure 4.** SEM images of the membrane surface structures of (A) PDMS-1, (B) PDMS-3, and (C) PDMS-5 at 500 $\times$  magnification. SEM images of the membrane surface structures of (a) PDMS-1, (b) PDMS-3, and (c) PDMS-5 at 10,000 $\times$  magnification. [Color figure can be viewed in the online issue, which is available at [wileyonlinelibrary.com](http://wileyonlinelibrary.com).]

crosslinking points, which increased the crosslinking density of the PDMS matrix. We also observed that the higher content of TEOS in the PDMS membrane led to a lower degree of membrane swelling. In general, the SD of the membrane decreased with increasing crosslinking density. The higher amounts of crosslinking points offered stronger elastic resistance, which led to a lower SD of the membranes.

**Mechanical Properties.** The testing results of the mechanical stability, including the tensile strength and strain at break, are listed in Table I. The mechanical stability of the membranes was enhanced with increasing TEOS content. This trend was interpreted by the strong interactions between the silica and PDMS

via the hydrogen bonds between the silanol groups on the silica surface and the oxygen atoms on the polymer chains. Silica was generated by the hydrolysis of TEOS, and the silica particles acted as crosslinking points in the composite membranes to link the polymeric chains and increase their rigidity; this indicated that more energy was needed to break down the bond between the silica and PDMS. As a result, the addition of a suitable amount of TEOS into the membranes improved the mechanical properties of the composite membranes. Li et al.<sup>36</sup> also observed the a mechanical stability for inorganic particles on PDMS membranes with similar trends.

#### Membrane Deoxygenation Performances

**Effect of the SiO<sub>2</sub> Content in the Hybrid Membranes.** The effect of the TEOS contents of the hybrid membrane on the oxygen–water permeability was investigated, as shown in Figure 6. The DO concentration in the feed water was kept at 9 mg/L, and the performed experiments had a duration time of 1 h. As shown in Figure 6, with increasing TEOS content, the separation factor of oxygen and water increased, and the  $J_o$  and  $J_w$  values of the hybrid membrane increased from PDMS-1 to PDMS-5. This was followed by a slight decrease when the TEOS–PDMS ratio was 0.6 (PDMS-6). With the TEOS–PDMS ratio increasing from 0.1 to 0.5, the oxygen flux increased from 1275 to 2182  $\text{mg}\cdot\text{m}^{-2}\cdot\text{h}^{-1}$  whereas the selectivity increased from 109.8 to 139.7. These figures indicate that not only the flux but also the separation factor were strongly dependent on the TEOS content.

The rubbery PDMS had great potential in the separation of gas and small molecules on the basis of the solution–diffusion mechanism. The diameters of oxygen and water molecules were

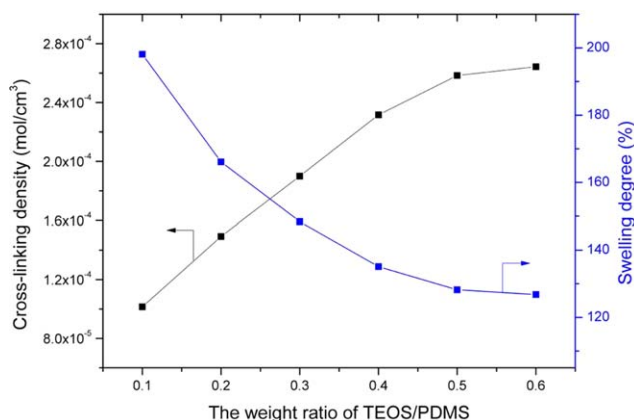


**Figure 5.** Effect of the TEOS content on the crosslinking density and the SD of the PDMS hybrid membranes. [Color figure can be viewed in the online issue, which is available at [wileyonlinelibrary.com](http://wileyonlinelibrary.com).]

**Table I.** Mechanical Properties of the Membranes

Membrane	Tensile strength (MPa)	Strain at break (%)
PDMS-1	5.63 ± 0.12	41.03 ± 0.86
PDMS-2	5.88 ± 0.15	50.70 ± 1.29
PDMS-3	6.92 ± 0.09	65.78 ± 0.89
PDMS-4	7.07 ± 0.16	67.48 ± 1.53
PDMS-5	7.39 ± 0.15	71.04 ± 1.44
PDMS-6	7.57 ± 0.13	74.85 ± 1.35

about 0.29 and 0.4 nm. Generally, smaller molecules (oxygen) diffused faster than larger molecules (water) because of a high fraction of free-volume voids available for smaller penetrant molecules. Moreover, the PDMS networks had excellent permeability to gas molecules; this was attributed to the high flexibility of the siloxane ( $-\text{Si}-\text{O}-$ ) chains, whereas water had a lower solubility and permeability because the PDMS chains contained  $-\text{Si}-\text{CH}_3$  groups, which made the PDMS membranes hydrophobic. Consequently, during the deoxygenation process, oxygen was the more permselective component through the membrane.

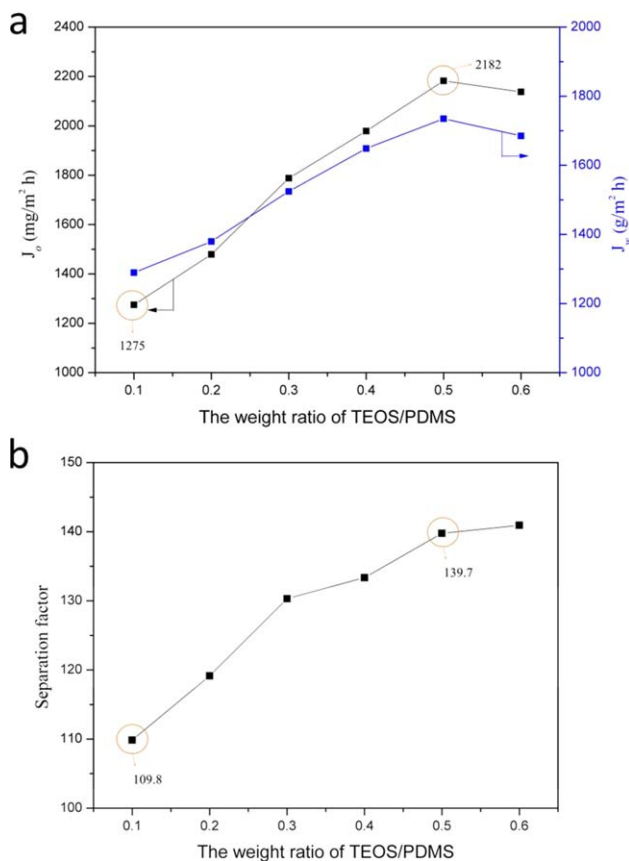


**Figure 6.** (a)  $J_o$  and  $J_w$  and (b) separation factor values with different TEOS contents (experimental conditions: DO concentration in feed water = 9 mg/L, operating temperature = 293 K, water flow rate = 160 L/h, vacuum level = 100 Pa, and operating time = 1 h). [Color figure can be viewed in the online issue, which is available at [wileyonlinelibrary.com](http://wileyonlinelibrary.com).]

In general, the permselectivity through mixed-matrix membranes strongly depends on their morphology: the volume fraction and the size and shape of the dispersed and continuous phases.<sup>42</sup> Smaller particles provide more polymer–particle interfacial area and enhance the polymer–filler interface contact. The incorporation of  $\text{SiO}_2$  particles into the PDMS matrix provided extra free volume to the polymer chains, enhanced the size of the network pores, and prevented the polymer chains from packing tightly; therefore, the oxygen and water molecules permeated more easily than they did through the pure PDMS membrane. On the other hand, when the concentration of silicon precursors increased, the PDMS mixed-matrix membranes offered more diffusion paths for those penetrant molecules. Consequently, the silica particles offered spaces for oxygen and water molecules to permeate through the membranes. However, when excessive silica particles were incorporated, the fractional free volume decreased accordingly; meanwhile, the mass-transfer resistance of the membrane increased, and this resulted in a negative effect on the permeability. These results show that the proper TEOS content was beneficial for oxygen permselectivity. A similar behavior was observed by Aroon et al.,<sup>26</sup> in which the introduction of inorganic fillers into PDMS significantly improved the properties of membranes because of the intermolecular interactions between inorganic and organic materials.

**Effect of the Operating Temperature.** The temperature is an important operating parameter in deoxygenation because it affects both the sorption and diffusion rates. The effects of the operating temperature for the vacuum degassing process through PDMS hybrid membranes are shown in Figure 7; the downstream absolute pressure was kept at 100 Pa, and the duration was 1 h. As shown in Figure 7(a),  $J_o$  slightly improved when the temperature was increased from 293 to 313 K, and  $J_w$  [Figure 7(b)] showed a visible increase. As a result, the separation factor decreased sharply [as shown in Figure 7(c)]. Both  $J_o$  and  $J_w$  increased at higher temperatures because of the higher partial pressures and high-frequency vibration of the polymer chains; these offered extra free volume within the polymer matrix and resulted in more molecules permeating the membrane. The diffusion rates of oxygen and water molecules were enhanced, and this led to a high permeation flux ( $J$ ). The concentration of water was much higher than that of oxygen in the feed solution; the increase in the feed temperature weakened the difference in the solubility and diffusion rates of oxygen and water molecules and caused a decrease in the separation factor.

The temperature dependence of  $J$  could be expressed by an Arrhenius relationship according to eq. (7):<sup>43</sup>

$$J = A_p \exp\left(\frac{-E_A}{RT}\right) \quad (7)$$

where  $A_p$  is a constant,  $E_A$  is the apparent activation energy for the permeation flux,  $T$  is the absolute temperature, and  $R$  is the gas constant.

Figure 8 shows Arrhenius plots ( $\ln J$  vs  $1/T$ ) through the PDMS membranes according to eq. (7). The temperature dependence of  $J$  agreed well with the Arrhenius relationship. The fitted apparent activation energies of the PDMS-5 membrane from

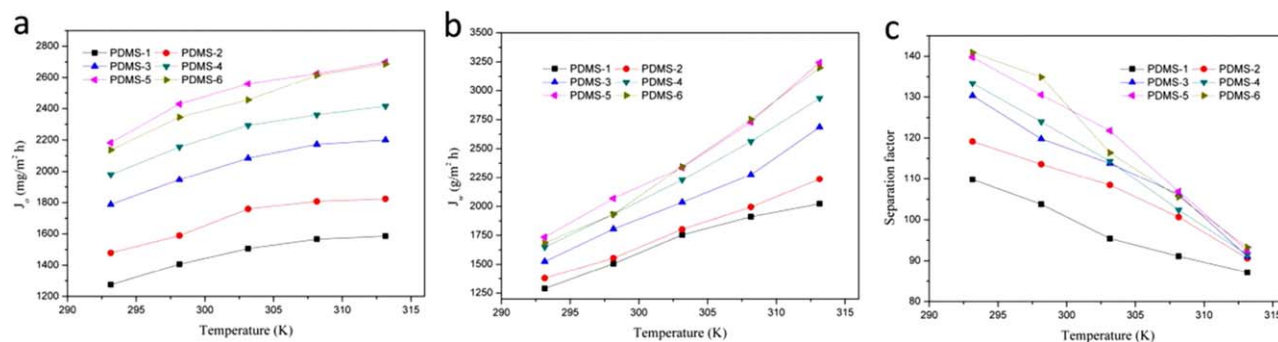


**Figure 7.** Effect of the operating temperature on the (a)  $J_o$ , (b)  $J_w$ , and (c) separation factor values with different TEOS contents (experimental conditions: DO concentration in feed water = 9 mg/L, water flow rate = 160 L/h, vacuum level = 100 Pa, and operating time = 1 h). [Color figure can be viewed in the online issue, which is available at [wileyonlinelibrary.com](http://wileyonlinelibrary.com).]

the slope were  $E_{\text{oxygen}} = 8.39$  kJ/mol and  $E_{\text{water}} = 21.71$  kJ/mol at a DO concentration of 9 mg/L; this indicated that the transport of oxygen molecules through the membrane occurred more readily than water under the operating temperature.

**Effect of the Operating Vacuum.** It is well known that the chemical potential difference between the permeate side and the feed side, which is created by the application of vacuum or a sweep gas to the permeate side of the membrane, is a critical mass-transfer driving force for the deoxygenation process. The operating vacuum is an important factor in the liquid–gas membrane separation process, and the effect of the operation of a vacuum on the oxygen-removal performances with the PDMS-5 membrane is revealed in Figure 9; the water flow rate was kept constant at 160 L/h with an operating temperature at 293 K and a running time of 1 h. The results show that  $J_o$  and  $J_w$  decreased as expected when the vacuum level (absolute pressure) in the downstream side of the apparatus increased from 100 Pa to 20 kPa. The vacuum applied underneath the membrane cell caused a drop in the oxygen partial pressure and provided the driving force for the degassing process. The  $J_o$  values were improved with an increase in the driving force. At a deeper vacuum level, the DO-removal efficiency increased, and this led to a high differential pressure of oxygen. Therefore, it was possible to achieve a higher DO-removal performance through a reduction in the absolute pressure. To achieve a superior removal performance, a deep vacuum level is needed.

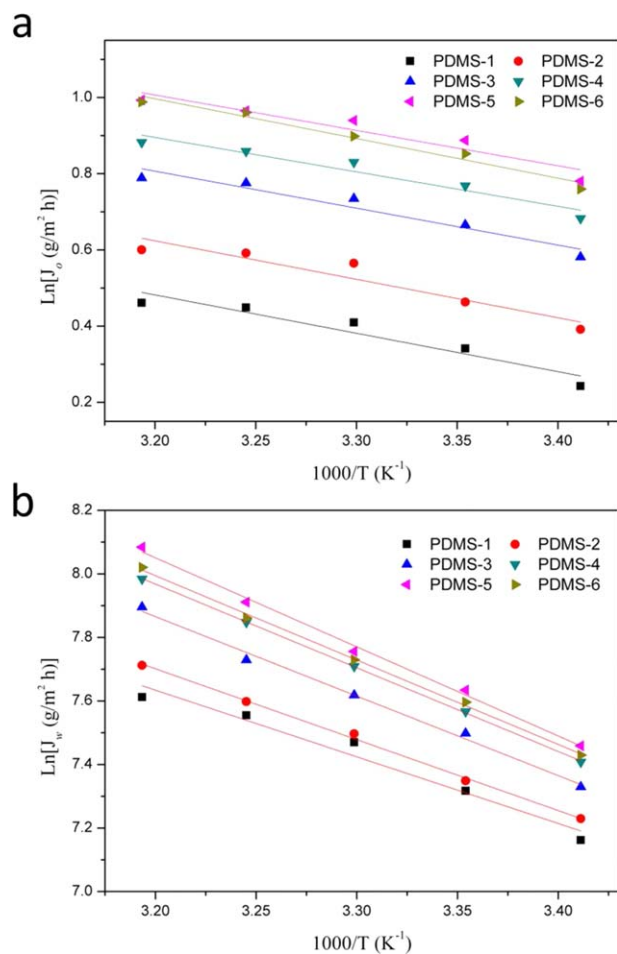


**Figure 8.** Temperature dependence of the (a)  $J_o$  and (b)  $J_w$  values (experimental conditions: DO concentration in feed water = 9 mg/L, water flow rate = 160 L/h, vacuum level = 100 Pa, and operating time = 1 h). [Color figure can be viewed in the online issue, which is available at [wileyonlinelibrary.com](http://wileyonlinelibrary.com).]

**Effect of the Water Flow Rate.** The effect of the water flow rate on the DO-removal performance with the PDMS-3 membrane is shown in Figure 10; the absolute pressure was kept at 100 Pa, and the operating temperature was maintained at 293 K with a running time of 1 h. The  $J$  values and the separation factor both increased measurably with the increase in the water flow rate up to 160 L/h and then slightly increased with the further increase in the water flow rate from 160 to 200 L/h. This may have been due to the decrease in the liquid film resistance in the liquid side of membrane at a higher water flow rate,<sup>44</sup> which promoted the mass transfer of both oxygen and water and resulted in an increase in the  $J$  values. Therefore, a higher oxygen-removal efficiency was obtained at a higher water flow rate. From an economic point of view, a water flow rate of 160 L/h was chosen for DO removal.

**Long-Term Experiment.** For industrial applications of vacuum degassing with a membrane process, it is expected that the level of DO concentration in water can be reduced to a low level by membrane module. PDMS-1 and PDMS-5 membranes were

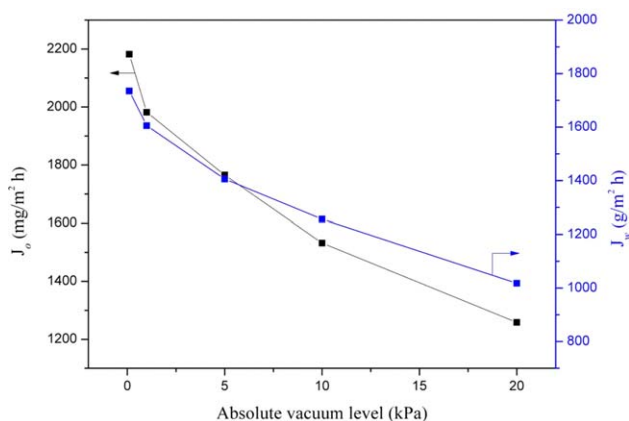


**Figure 9.** Effect of the operating vacuum on the oxygen-removal performance with the PDMS-5 membrane (experimental conditions: DO concentration in feed water = 9 mg/L, operating temperature = 293 K, water flow rate = 160 L/h, and operating time = 1 h). [Color figure can be viewed in the online issue, which is available at [wileyonlinelibrary.com](http://wileyonlinelibrary.com).]

tested in a long-term deoxygenation experiment. Figure 11 shows the oxygen concentration for a prolonged duration while the feed flow rate was kept at 160 L/h, the operating temperature was 293 K, and the vacuum level was 100 Pa. The DO con-

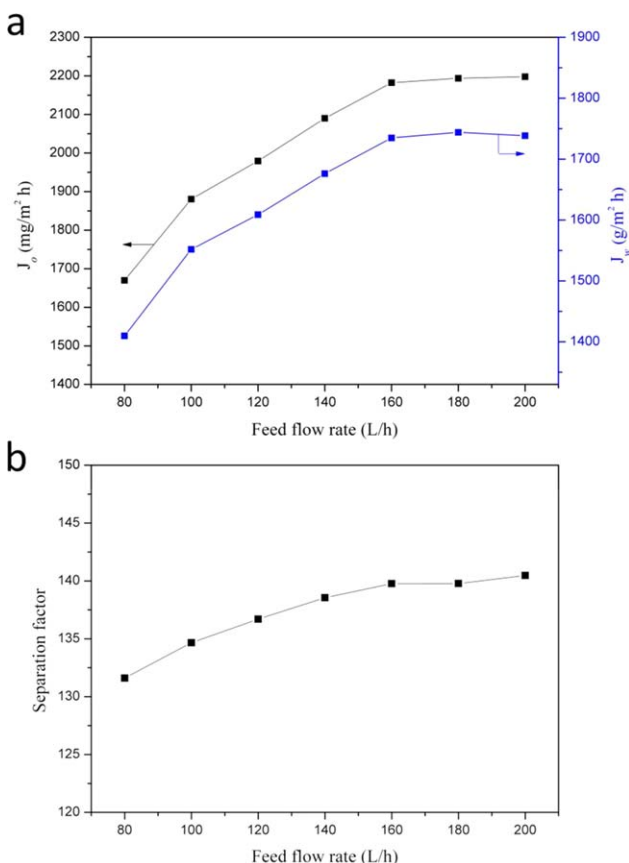


**Figure 10.** Effect of the water flow rate on the (a)  $J_o$  and  $J_w$  and (b) separation factor values with the PDMS-5 membrane (experimental conditions: DO concentration in feed water = 9 mg/L, operating temperature = 293 K, vacuum level = 100 Pa, and operating time = 1 h). [Color figure can be viewed in the online issue, which is available at [wileyonlinelibrary.com](http://wileyonlinelibrary.com).]

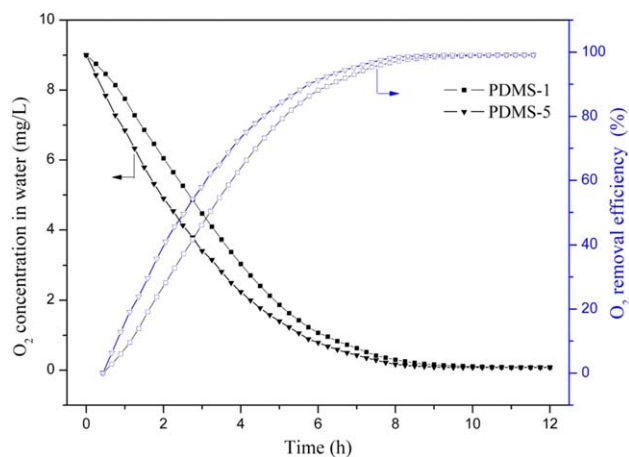


**Figure 11.** Effect of the long-term operating time with PDMS-1 and PDMS-5 (experimental conditions: DO concentration in feed water = 9 mg/L, operating temperature = 293 K, water flow rate = 160 L/h, and vacuum level = 100 Pa). [Color figure can be viewed in the online issue, which is available at [wileyonlinelibrary.com](http://wileyonlinelibrary.com).]

centration of the two membranes decreased to the same value of 0.015 mg/L finally, and the DO-removal efficiency was 99.8%. According to the mass-transfer model, oxygen transport through the membrane was achieved through maintenance of a lower pressure on the permeate side of the membrane. Figure 11 also shows that the equilibrium time of PDMS-5 was shorter than that of PDMS-1; this suggested that the PDMS mixed-matrix membrane showed enhanced productivity and efficiency. The PDMS membrane has good potential to improve performance in industrial degassing applications.

## CONCLUSIONS

In this study, the fabrication of mixed-matrix membranes was carried out with TEOS and siloxane polymers via the sol-gel process. Hydroxyl-terminated siloxane polymers were reactive enough to be incorporated into the silica networks. Silica particles were generated *in situ* by the hydrolysis reaction of TEOS. The membrane properties and morphological structure were characterized, and the crosslinking density was measured.

The results indicate that the introduction of TEOS sol affected the morphologies and properties significantly. The hybrid membranes improved the oxygen-removal efficiency remarkably, and a maximum  $J$  was obtained when the weight ratio of PDMS to TEOS was 10:5. An improved PDMS membrane was obtained, and it enhanced the DO-removal performance through the control of the TEOS concentration in the PDMS mixed-matrix membranes.

The effects of the operating parameters, such as the water temperature, operating vacuum, and water flow rate, were also investigated. A low temperature enhanced the membrane performance. The lower absolute pressure applied to the membrane was a very suitable method for removing DO from water. The results show that this kind of composite membrane efficiently removed DO, and the silica particles could be formed *in situ* and homogeneously embedded into the polymer matrix to render membranes with tunable free-volume properties and superior separation performance. This high-performance



separation PDMS membrane showed great potential in the deoxygenation process.

## ACKNOWLEDGMENTS

This work was supported by the Plan of National Science and Technology Support Program (contract grant number 2012BAC02B03) and the Fundamental Research Funds for the Central Universities of China (award 2012203020213).

## REFERENCES

1. Ito, A.; Yamagiwa, K.; Tamura, M.; Furusawa, M. *J. Membr. Sci.* **1998**, *145*, 111.
2. Yagi, Y.; Imaoka, T.; Ksama, Y.; Ohmi, T. *IEEE Trans. Semicond. Manuf.* **1992**, *5*, 121.
3. Tan, X.; Li, K. *Chem. Eng. Sci.* **2000**, *55*, 1213.
4. Van der Vaart, R.; Lebedeva, V. I.; Petrova, I. V. *J. Membr. Sci.* **2007**, *299*, 38.
5. Moon, J. S.; Park, K. K.; Kim, J. H. *Appl. Catal. A* **2000**, *201*, 81.
6. Chua, I.; Tai, M. S. L.; Li, K.; Zhang, H.; Sourirajan, S.; Ng, W. J.; Teo, W. K. *IES J.* **1993**, *3*, 57.
7. Li, K.; Chua, I.; Ng, W. J.; Teo, W. K. *Chem. Eng. Sci.* **1995**, *50*, 3547.
8. Ismail, A. F.; Mansourizadeh, A. *J. Membr. Sci.* **2010**, *365*, 319.
9. Martić, I.; Maslarević, A.; Mladenović, S. *Desalination Water Treat.* **2014**, *1*, 5.
10. Hashim, S. M.; Mohamed, A. R.; Bhatia, S. *Adv. Colloid Interfaces* **2010**, *160*, 88.
11. Awanis Hashim, N.; Liu, Y.; Li, K. *Chem. Eng. Sci.* **2011**, *66*, 1565.
12. Zhang, Q.; Cussler, E. L. *J. Membr. Sci.* **1985**, *23*, 333.
13. Malek, A.; Li, K.; Teo, W. K. *Ind. Eng. Chem. Res.* **1997**, *36*, 784.
14. Kreulen, H.; Smolders, C. A.; Versteeg, G. F.; Van Swaaij, W. P. M. *J. Membr. Sci.* **1993**, *78*, 217.
15. Karoor, S.; Sirkar, K. *Ind. Eng. Chem. Res.* **1993**, *32*, 674.
16. Vladisavljevic, G. T. *Sep. Purif. Technol.* **1999**, *17*, 1.
17. Li, T.; Yu, P.; Luo, Y. *J. Appl. Polym. Sci.* **2014**, *131*, 40430.
18. Leiknes, T.; Semmens, M. *J. Sep. Purif. Technol.* **2001**, *22*, 287.
19. Peng, Z. G.; Lee, S. H.; Zhou, T.; Shieh, J. J.; Chung, T. S. *Desalination* **2008**, *234*, 316.
20. Bhaumik, D.; Majumdar, S.; Kamalesh, Q. F.; Sirkar, K. *J. Membr. Sci.* **2004**, *235*, 31.
21. Gabelman, A.; Hwang, S. *J. Membr. Sci.* **1999**, *159*, 61.
22. Aoki, T. *Prog. Polym. Sci.* **1999**, *24*, 951.
23. Nunes, S. P.; Peinemann, K. V.; Ohlogge, K.; Alpers, A.; Keller, M.; Pires, A. T. N. *J. Membr. Sci.* **1999**, *157*, 219.
24. Mark, J. E. *Acc. Chem. Res.* **2004**, *37*, 946.
25. Nguyen, Q. T.; Nobe, K. *J. Membr. Sci.* **1987**, *30*, 11.
26. Aroon, M. A.; Ismail, A. F.; Matsuura, T. *Sep. Purif. Technol.* **2010**, *75*, 229.
27. Liu, G.; Wei, W.; Wu, H.; Dong, X.; Jiang, M.; Jin, W. *J. Membr. Sci.* **2011**, *373*, 121.
28. Zhou, H.; Su, Y.; Chen, X.; Yi, S.; Wan, Y. *Sep. Purif. Technol.* **2010**, *75*, 286.
29. Li, B.; Yu, S.; Jiang, Z.; Liu, W.; Cao, R.; Wu, H. *J. Hazard. Mater.* **2012**, *211*, 296.
30. Sohoni, G. B.; Mark, J. E. *J. Appl. Polym. Sci.* **1992**, *45*, 1763.
31. Bansal, A.; Yang, H.; Li, C. *Nat. Mater.* **2005**, *4*, 693.
32. Merkel, T. C.; Freeman, B. D.; Spontak, R. *J. Science* **2002**, *296*, 519.
33. Peng, F.; Lu, L.; Sun, H. *Chem. Mater.* **2005**, *17*, 6790.
34. Balazs, A. C.; Emrick, T.; Russell, T. P. *Science* **2006**, *314*, 1107.
35. Chen, H. Y.; Ruckenstein, E. *J. Chem. Phys.* **2009**, *131*, 244904.
36. Li, B.; Liu, W.; Wu, H. *J. Membr. Sci.* **2012**, *415*, 278.
37. Duo, S.; Li, M.; Zhu, M. *Mater. Chem. Phys.* **2008**, *112*, 1093.
38. Shao, J.; Liu, H.; He, Y. *Desalination* **2008**, *234*, 370.
39. Leiknes, T. O.; Semmens, M. *J. Sep. Purif. Technol.* **2001**, *22*, 287.
40. Li, K.; Tan, X. *Chem. Eng. Sci.* **2001**, *56*, 5073.
41. Flory, P. J.; Rabjohn, N.; Shaffer, M. C. *J. Polym. Sci.* **1949**, *4*, 225.
42. Li, X. G.; Kresse, I.; Springer, J. *Polymer* **2001**, *42*, 6859.
43. Xiangli, F.; Chen, Y.; Jin, W. *Ind. Eng. Chem. Res.* **2007**, *46*, 2224.
44. Naim, R.; Ismail, A. F.; Mansourizadeh, A. *J. Membr. Sci.* **2012**, *392*, 29.